

**Composition and local atomic arrangement of decagonal Al-Co-Cu quasicrystal surfaces**R. Zenkyu,<sup>1</sup> J. Yuhara,<sup>1</sup> T. Matsui,<sup>1</sup> S. Shah Zaman,<sup>2</sup> M. Schmid,<sup>2</sup> and P. Varga<sup>2</sup><sup>1</sup>*School of Engineering, Nagoya University, Furo-cho, Chikusa-ku, Nagoya, 464-8603, Japan*<sup>2</sup>*Institut für Angewandte Physik, Technische Universität Wien, Vienna, Austria*

(Received 7 December 2011; revised manuscript received 30 July 2012; published 17 September 2012)

We investigated the composition of decagonal Al-Co-Cu surface by Auger electron spectroscopy (AES) and low-energy ion scattering (LEIS). The surface composition after annealing was Al richer and Co poorer compared to that after sputtering or bulk composition. Two types of the characteristic clusters were observed by scanning tunneling microscopy (STM) and no bias voltage dependence of the image was observed. On the other hand, scanning tunneling spectroscopy revealed a subtle difference of local density of states in unoccupied states between different sites. Structural optimization using *ab initio* calculations based on density functional theory (DFT) was performed on several compositional models, which are based on the W-(AlCoNi) bulk model. The surface structures of two types of the characteristic clusters were determined by comparison of the STM image and the simulated image of the structures obtained by DFT. The topmost layer was composed of Al and Cu atoms, and the compositional ratio was consistent with the AES and LEIS results.

DOI: [10.1103/PhysRevB.86.115422](https://doi.org/10.1103/PhysRevB.86.115422)

PACS number(s): 61.44.Br, 68.37.Ef, 68.35.Dv, 71.15.Nc

**I. INTRODUCTION**

A few decades ago, quasicrystals (QC) were discovered by Shechtman as a new type of solid.<sup>1</sup> It was found that quasicrystals can be thermodynamically stable,<sup>2,3</sup> and their atomic arrangement has been scrutinized by single-grain x-ray diffraction analysis (XRD), high-resolution transmission electron microscopy (HRTEM), convergence beam electron diffraction (CBED), scanning transmission electron microscopy (STEM), and other techniques. Since a QC structure in two-dimensional (2D) or three-dimensional (3D) space can be obtained by projection from a structure with a higher dimension, the determination of the atomic arrangement is equivalent to the determination of an occupation domain in a high-dimensional periodic space. While much effort has been devoted to the determination of the bulk structures of quasicrystals, much less is known about their surface structures.

Studies of 2D quasicrystal have mainly focused on decagonal (d-) Al-Co-Ni and d-Al-Co-Cu quasicrystals.<sup>4</sup> For the 2D quasicrystals, HRTEM and STEM are successful methods to directly identify the atomic arrangement in real space.<sup>5-12</sup> In particular, STEM has been drastically improved in that the diameter of the scanning electron beam became smaller than an atomic radius; therefore, the collaboration of XRD and STEM has attracted a great deal of attention to identify the atomic arrangement of 2D quasicrystals.<sup>13,14</sup> The d-Al-Co-Ni quasicrystals show several stable quasiperiodic phases, with different Co:Ni ratios.<sup>15</sup> On the other hand, d-Al-Co-Cu quasicrystals show a single stable decagonal phase.<sup>16-18</sup>

Studies of d-Al-Co-Cu using the atom location by channeling-enhanced microanalysis (ALCHEMI) method showed that the Co and Cu sites are well ordered and occupy different sublattices, whereas it was found that the Co and Ni sites are randomly disordered in Co-rich d-Al-Co-Ni.<sup>19</sup> These results indicate that there are different stabilization mechanisms in d-Al-Co-Ni and d-Al-Co-Cu. Monte Carlo simulations also indicate that the strong chemical ordering of Co and Cu is important for the quasiperiodicity of d-Al-Co-Cu.<sup>20</sup>

Concerning the atomic arrangement in 2-nm clusters of d-Al<sub>65</sub>Co<sub>20</sub>Cu<sub>15</sub>, it has been proposed by XRD that the decagonal structure is composed of two equivalent quasiperiodic layers, related by a 36° rotation, and ABAB stacking, resulting in a tenfold rotational symmetry of the crystal.<sup>13</sup> Recently, the atomic arrangement in 2-nm columnar clusters of d-Al<sub>64</sub>Co<sub>22</sub>Cu<sub>14</sub> has been directly observed by STEM, showing that the atomic arrangement in the 2-nm clusters has fivefold, not tenfold symmetry.<sup>12</sup> The structure of d-Al-Co-Cu has been shown to be close to that of the W-(AlCoNi) approximant crystal, except for occasional exchange of Al and TM (transition metal) atoms around the cluster centers in d-Al-Co-Cu.<sup>12</sup> The structural model of the W-(AlCoNi) crystalline approximant has been determined by XRD to be two inequivalent layers, the flat A and the puckered B layer.<sup>21</sup> Therefore, the W-(AlCoNi) structural model is very useful for density functional theory (DFT) calculations to determine the atomic arrangement of d-Al-Co-Cu quasicrystals, similar to the previous DFT studies of the Al-Co-Ni quasicrystals.<sup>22,23</sup>

The surface structures of d-Al-Co-Ni and d-Al-Co-Cu have been studied by scanning tunneling microscopy (STM), showing several types of clusters with fivefold symmetry on the surface.<sup>24-30</sup> However, a structural model has not been obtained because of the difficulty to determine the surface composition quantitatively. So far, the surface composition of a Co-rich d-Al-Co-Ni quasicrystal has been investigated by Auger electron spectroscopy (AES) and low-energy ion scattering (LEIS), indicating that Al atoms segregate to the surface on annealing.<sup>26</sup> Another AES study came to the conclusion that the surface concentration after annealing was the same as a cleaved surface.<sup>31</sup> In that study, however, the high-energy 1396-eV Al *KLL* line was used, which implies a low sensitivity to the surface concentration compared to low-energy AES lines or LEIS. The surfaces of d-Al-Co-Ni have been also examined by low-energy electron diffraction (LEED)-IV analysis, where only truncated-bulk models were considered.<sup>32-34</sup> Assuming the structure of the W-(AlCoNi) approximant, it was found that the Al-rich B layer of the

approximant results in a better agreement with experiment than the TM-rich A layer models.<sup>34</sup> LEED-IV must be considered problematic for this application, however, as it has been shown that LEED-IV studies of alloys comprising Al and 3d transition metals suffer from strong coupling between the composition and Debye Waller factor (which includes static disorder, certainly present in QCs).<sup>35</sup> In Ref. 23, simulated STM images of the bulk-terminated W-(AlCoNi) approximant have been compared to experimental images of d-Al-Co-Ni.<sup>26</sup> Only partial agreement was found, with some local fivefold clusters in the STM image similar to the simulation of the Al-rich B layer; others were interpreted as comparable to sites in the TM-rich A layer. In summary, no clear picture arises for the composition and structure of these surfaces, and it is still controversial whether Al segregation or a truncated bulk structure describes the surface.

In our previous study, we have shown characteristic clusters on the d-Al-Co-Cu surface by STM.<sup>29</sup> We have shown that each layer has only fivefold, not tenfold symmetry, and that the characteristic fivefold clusters become rotated by  $36^\circ$  (inverted) when ascending or descending one  $\sim 2\text{-\AA}$  terrace level. This observation agrees with several models having equivalent (but inverted) adjacent layers.<sup>13,36</sup> The model of Burkov<sup>36</sup> is based on clusters with a 2-nm diameter and pentagonal symmetry. In our STM images, two types of smaller pentagonal clusters were identified as forming the corners of the 2-nm clusters. While the atomic arrangements of the A and B layers of the W-(AlCoNi) approximant are different, and also electron microscopy data suggest inequivalent A and B layers,<sup>6,9-12</sup> STM images of two adjacent terraces, which should correspond to the A and B layer, show the same structure, apart from the opposite orientation of the clusters.<sup>29</sup> Also, we did not observe alternating large and small terraces, which indicates that we do not have two significantly different surface structures with different surface energies. This may indicate that either there is no significant difference between A and B layers in the bulk (apart from the  $36^\circ$  rotation, as in the models of Refs. 13 and 36) or that the surface structure is different from the bulk and not significantly affected by the difference between an A and B layer below. Very recently, Schaub *et al.* have studied d-Al-Co-Cu by x-ray diffraction and present a new model with a four-layer periodicity along  $z$ , but only alternating layers are structurally different (flat and puckered).<sup>37</sup> Based on the three-dimensional pair distribution function, they also concluded that the lateral correlation between the columnar units is weak for d-Al-Co-Cu, which can imply that the surface structures of two adjacent terraces can be equivalent when averaged over larger areas.<sup>37</sup>

In this paper, we present a combined experimental and computational study on the d-Al-Co-Cu surface. We study the surface structure and composition by means of low-energy electron diffraction (LEED), AES, LEIS, STM, and scanning tunneling spectroscopy (STS). We also draw conclusions on the atomic arrangement of the two types of the characteristic clusters from a comparison of experimental STM and simulated STM images obtained by DFT.

## II. EXPERIMENT AND CALCULATION

The experiment was performed using two very similar ultrahigh-vacuum systems in Nagoya and Vienna. Each system consisted of a preparation chamber with a base pressure below  $2 \times 10^{-10}$  mbar, and an analysis chamber with a base pressure below  $10^{-10}$  mbar. Single-grain d-Al-Co-Cu quasicrystals were used in the present experiment. High-resolution STM, STS, and LEED were performed on a d-Al<sub>66</sub>Co<sub>17</sub>Cu<sub>17</sub> surface prepared by the Bridgman method<sup>38</sup> and a d-Al<sub>65</sub>Co<sub>20</sub>Cu<sub>15</sub> surface prepared by the Czochralski method.<sup>39</sup> The latter sample was also used for the AES and LEIS studies. Both samples were cut perpendicular to the tenfold axis and polished with 0.25- $\mu\text{m}$  diamond paste.

Clean surfaces were prepared by 2-keV Ar<sup>+</sup> ion sputtering at room temperature followed by annealing the sample up to 800 °C or 880 °C. The sample temperature was monitored by a radiation thermometer and a type-K thermocouple mounted on the base plate of the sample holder. The cleanliness of the surface was measured by AES after sputtering and annealing; no contaminants such as C and O were observed within the detection limits.

The LEED, STM, and STS experiments were conducted at Nagoya University in an UHV chamber equipped with a customized Omicron room temperature STM (STM-1), and four-grid LEED optics. STM images were obtained in constant current mode. STS spectra were obtained with a setpoint of +0.5 V/0.3 nA. For each characteristic position, more than 15 spectra of equivalent sites were obtained and averaged. We have taken care to exclude spectra where the tip was unstable.

The AES and LEIS experiments were performed at Technische Universität Wien in an UHV chamber equipped with a customized Omicron room-temperature micro-STM, a cylindrical mirror analyzer with coaxial electron gun (3 keV) for AES, and an ion source and hemispherical analyzer for LEIS. The elemental concentrations in the surfaces were estimated from converting the AES peak-to-peak heights into concentrations, based on the sensitivity factors 0.23 for Al (68 eV), 0.26 for Co (775 eV), and 0.21 for Cu (920 eV).<sup>40</sup> Since the Al *LMM* (68 eV) peak partially overlaps with the Cu *MNN* (60 eV), the Al peak-to-peak height was estimated from the difference between the minimum and the baseline of the differentiated Al signal. This procedure reduces the influence of the Cu peak, which is at lower energy and thus mainly influences the maximum of the differentiated signal. Similarly, the Co *LMM* (775 eV) peak overlaps with the Cu *LMM* (778 eV) peak, thus, the Co peak-to-peak height at 775 eV was calculated from the Co peak-to-peak height at 716 eV and the ratio of these peaks was measured on a pure Co sample. The escape depths at perpendicular emission are  $\sim 0.26$ , 1.21, and 1.49 nm for the Al, Co, and Cu peaks, respectively.<sup>41,42</sup>

The surface densities (atoms per unit area) and concentrations of Al, Co, and Cu in the topmost and second layers were estimated from the LEIS spectra compared to those of standard samples, Al(111), Co(0001), and Cu(111), which were cleaned by cycles of 2-keV Ar<sup>+</sup> sputtering at room temperature followed by annealing for 10 min at 400 °C, 300 °C, and 500 °C, respectively. In the LEIS experiments,

a 1-keV  $\text{He}^+$  ion beam was incident at the angle of  $45^\circ$  and the scattered  $\text{He}^+$  ions were detected at a scattering angle of  $90^\circ$ .

The approximant used for our DFT studies was based on the W-(AlCoNi) structure, which is justified by the similarity of the 2-nm clusters in d-Al-Co-Cu found by STEM.<sup>12</sup> Therefore, we have replaced the Ni atoms in the W-(AlCoNi) bulk model by Cu, creating a W-(AlCoCu) structure. The W-(AlCoNi) bulk model, with stacking sequence A, B, A', B, was taken from No. 92 in the Mihalkovič database.<sup>43</sup> To reduce the computational effort, our model was built by cutting the W-(AlCoCu) cell perpendicular to the  $a$  axis in half, resulting in  $a = 19.88 \text{ \AA}$ ,  $b = 23.39 \text{ \AA}$ . In the  $c$  direction, we have used four layers with the two bottom layers frozen and 10- $\text{\AA}$  vacuum. The structural optimization has been performed with DFT using the Vienna *ab initio* simulation package (VASP),<sup>44</sup> using the projector augmented wave (PAW) method<sup>45</sup> and generalized gradient approximation with a plane-wave cutoff of 250 eV.<sup>46</sup> Residual forces were smaller than 0.02 eV/ $\text{\AA}$ . STM simulations were performed by DFT and the Tersoff-Hamann approach.<sup>47</sup>

### III. RESULTS AND DISCUSSION

#### A. Experiments

Figure 1 shows the LEED pattern of the d- $\text{Al}_{65}\text{Co}_{20}\text{Cu}_{15}$  surface after the cycles of sputtering and annealing. Since the LEED pattern showed sharp spots with tenfold symmetry at  $\tau$  scaling distances (approximately 1:1.618), the well-ordered quasiperiodic surface was obtained, as in our previous study of d- $\text{Al}_{66}\text{Co}_{17}\text{Cu}_{17}$  tenfold surface.<sup>29</sup> It was confirmed that both of the annealing temperatures of  $800^\circ\text{C}$  and  $880^\circ\text{C}$  were high enough to form the tenfold quasiperiodic surface.

Figure 2 shows the AES spectra of the d- $\text{Al}_{65}\text{Co}_{20}\text{Cu}_{15}$  surfaces after sputtering and annealing at  $800^\circ\text{C}$  and  $880^\circ\text{C}$ . Using the procedure described above, we found a surface composition after sputtering of  $\text{Al}_{62}\text{Co}_{25}\text{Cu}_{13}$ , which is more Co rich than the bulk. As sputtering will destroy the QC order, one should expect segregation in the altered layer based on surface energies, i.e., Al segregating to the surface of the altered layer, irrespective of whether annealed QCs have a bulk-terminated surface after annealing or not. This effect

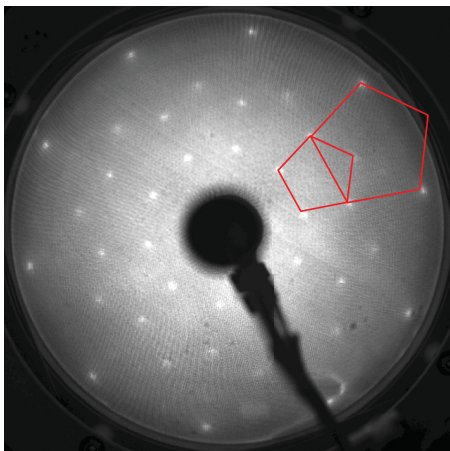


FIG. 1. (Color online) LEED pattern of the d- $\text{Al}_{65}\text{Co}_{20}\text{Cu}_{15}$  tenfold surface at 60 eV electron energy. The quasiperiodicity is illustrated with pentagons.

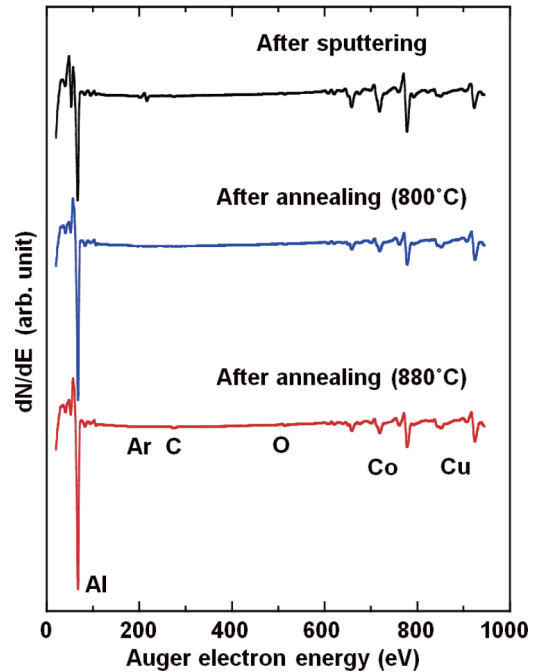


FIG. 2. (Color online) AES spectra of d- $\text{Al}_{65}\text{Co}_{20}\text{Cu}_{15}$  surfaces after sputtering and after annealing at  $800^\circ\text{C}$  and  $880^\circ\text{C}$ .

will be superimposed on the Al depletion due to preferential sputtering.<sup>48–50</sup> Because of the highly surface-sensitive low-energy AES line of Al, the present result should be significantly influenced by the Al segregation to the top; the Al concentration in the subsurface layers is, of course, lower. The surface composition after annealing was obtained as  $\text{Al}_{77}\text{Co}_{10}\text{Cu}_{13}$ . It was confirmed that there was no difference between the AES spectra after annealing at  $800^\circ\text{C}$  and  $880^\circ\text{C}$ . Compared to the bulk composition or the surface composition after sputtering, after annealing, the surface is Al rich and Co poor.

The composition of the uppermost layer(s) of d- $\text{Al}_{65}\text{Co}_{20}\text{Cu}_{15}$  was also examined using LEIS, which is a very surface-sensitive technique. Figure 3(a) shows the LEIS spectra of the standard samples of Al(111), Co(0001), and Cu(111). The surface densities of Al(111), Co(0001), and Cu(111) are  $1.41 \times 10^{15}$  atoms/ $\text{cm}^2$ ,  $1.83 \times 10^{15}$  atoms/ $\text{cm}^2$ , and  $1.77 \times 10^{15}$  atoms/ $\text{cm}^2$ , respectively. Figures 3(b) and 3(c) show the LEIS spectra of the d- $\text{Al}_{65}\text{Co}_{20}\text{Cu}_{15}$  surfaces after sputtering and after annealing at  $880^\circ\text{C}$ . The LEIS spectra after annealing at  $800^\circ\text{C}$  were very similar to those at  $880^\circ\text{C}$ . We obtained the surface densities by comparison between the LEIS spectra of the d- $\text{Al}_{65}\text{Co}_{20}\text{Cu}_{15}$  surface and the standard samples, Al(111), Co(0001), and Cu(111), without considering any matrix effects.<sup>51</sup> The resulting Al, Co, and Cu densities in the d- $\text{Al}_{65}\text{Co}_{20}\text{Cu}_{15}$  surface after sputtering are  $8.9 \times 10^{14}$ ,  $1.0 \times 10^{14}$ , and  $1.6 \times 10^{14}$  atoms/ $\text{cm}^2$ , respectively, while those after annealing are  $14.0 \times 10^{14}$ ,  $0.3 \times 10^{14}$ , and  $1.4 \times 10^{14}$  atoms/ $\text{cm}^2$ , respectively. For comparison, in the bulk the average layer densities are  $8.8 \times 10^{14}$ ,  $2.0 \times 10^{14}$ , and  $2.7 \times 10^{14}$  atoms/ $\text{cm}^2$  for Al, Co, and Cu, respectively. These LEIS results indicate that annealing induces Al segregation to the surface; the Co surface concentration decreases, while

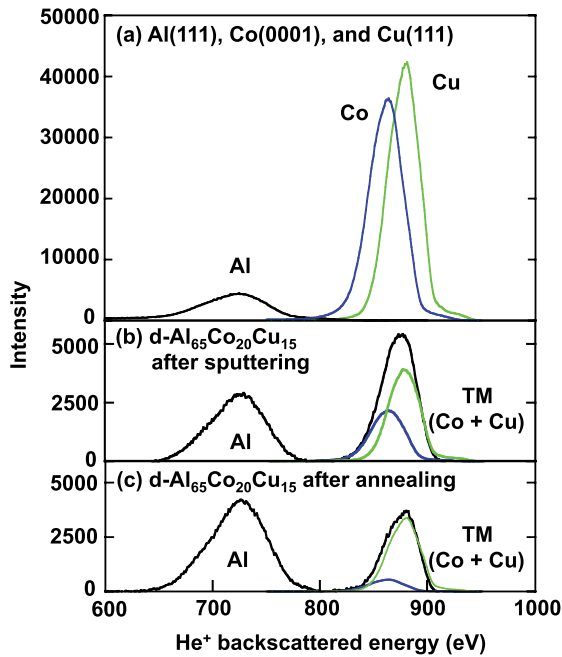


FIG. 3. (Color online) LEIS spectra of (a) standard samples of Al(111), Co(0001), and Cu(111), and a  $d\text{-Al}_{65}\text{Co}_{20}\text{Cu}_{15}$  surface, (b) after sputtering and (c) after annealing at  $880^\circ\text{C}$ .

the Cu surface concentration does not change significantly. The concentration changes obtained by LEIS qualitatively agree with those estimated from AES. The observation of Al enrichment and Co depletion also agrees with the expected surface segregation, considering that Al has the lowest and Co the highest surface energy of the three alloy constituents.

Figures 4(a) and 4(b) show STM images of the  $d\text{-Al}_{66}\text{Co}_{17}\text{Cu}_{17}$  surfaces at sample bias voltages of 0.5 and  $-0.3$  V, respectively. The images of the  $d\text{-Al}_{65}\text{Co}_{20}\text{Cu}_{15}$  sample are very similar (not shown). The solid and broken lines indicate two types of the dominant clusters at the surface that have been named G and Y cluster in our previous study.<sup>29</sup> These STM images show no strong bias voltage dependence; the appearance of the G and Y clusters is similar at positive and negative voltage. Therefore, each bright spot in the cluster seems to correspond to a single atom or a very small group of atoms. The smaller circles indicate  $\sim 0.1$ -nm-high protrusions, which tend to be observed mainly at the edge of Y clusters. Similar protrusions were also observed on the  $d\text{-Al-Co-Ni}$  surface and attributed to impurities, e.g., oxide clusters.<sup>26</sup>

We have studied these high protrusions and the center of two types of the clusters in Fig. 4(a) by STS to investigate their local density of states (LDOS). Figure 5 shows the STS spectra of the protrusions and the G and Y clusters. Positive sample bias represents unoccupied states and negative sample bias represents occupied states. All the STS spectra are qualitatively similar and have a shoulder at the bias voltage of 0.3 eV. The STS spectra of the 0.1-nm-high protrusions for the  $d\text{-Al-Co-Cu}$  are very different from those for the  $d\text{-Al-Co-Ni}$ . As all the STS spectra are similar in the  $d\text{-Al-Co-Cu}$  case, we do not attribute these protrusions to oxide but rather to metallic clusters.

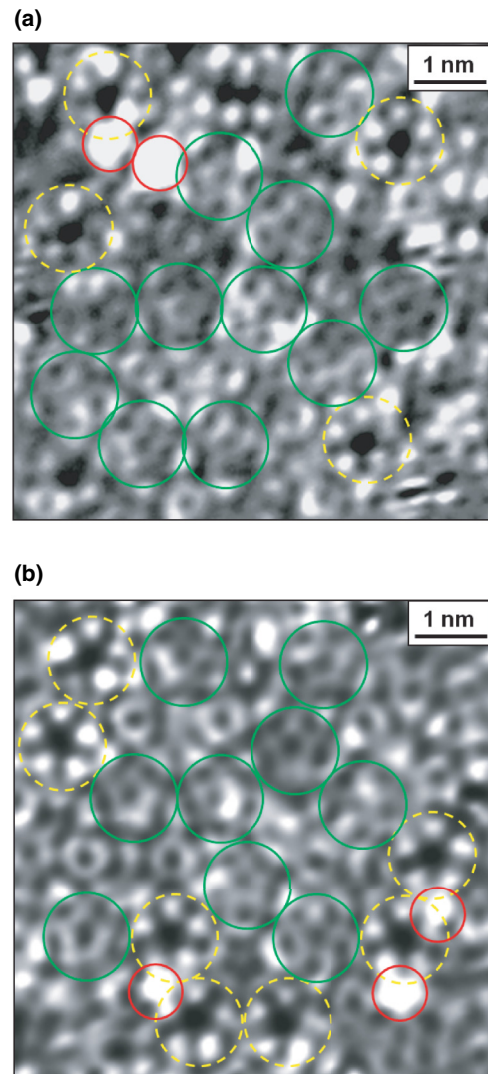


FIG. 4. (Color online) STM images of the  $d\text{-Al-Co-Cu}$  surface (a) positive ( $V_s = 0.5$  V,  $I_t = 0.3$  A) and (b) negative sample bias ( $V_s = -0.3$  V,  $I_t = 1.0$  A).

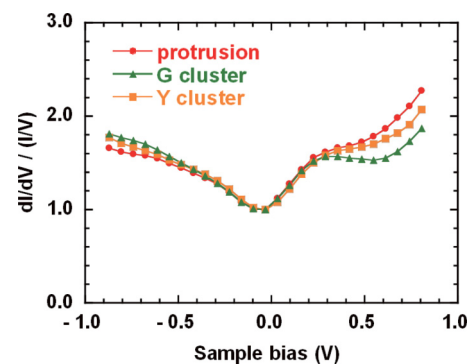


FIG. 5. (Color online) STS spectra of the 0.1-nm-high protrusions and the G and Y clusters of the  $d\text{-Al-Co-Cu}$  surface, indicated by circles, triangles, and squares, respectively.

### B. Computational results

DFT calculations were performed for more than 15 different W-(AlCoCu) surface models. Apart from the bulk-terminated models, we have only considered models with surface enrichment of Al and depletion of Co, as observed by AES and LEIS. We have put focus especially on the fivefold clusters at the corners of the 2-nm clusters, which have a prominent role in the STM images (G and Y clusters; cf. Ref. 29). Figure 6 shows such a model, which turned out to be the one fitting the experimental STM images. Figure 6(a) shows the bulk W-(AlCoCu) approximant. Two 2-nm clusters are marked with red circles. Figures 6(b) and 6(c) show the original A layer and its modification. The Al, Co, and Cu atoms are represented with different diameter (Al atoms are larger) and different brightness/color (silver, blue, and green, respectively). In constructing an initial model, all transition metal atoms in the topmost layer were removed and the Al atoms of the pentagonal cluster indicated by the arrows in Fig. 6(b) were replaced with Cu atoms, as shown in Fig. 6(c). Figures 6(d) and 6(e) show the top and side views of the W-(AlCoCu) initial state of this model before relaxation by DFT. The topmost layer in this model is the modified A layer. The other three layers (B, A', and B layers) are the same as the original. The composition of this model (all four layers) is  $\text{Al}_{76}\text{Co}_{12}\text{Cu}_{12}$ , which is close to the estimate from AES,  $\text{Al}_{77}\text{Co}_{10}\text{Cu}_{13}$ . Since we have a rather open surface, LEIS will see a contribution of the second layer. When neglecting matrix

effects, we can assume that the contribution of the first layer is 100%, i.e., each atom contributes to the LEIS spectrum as much as an atom in the respective standard. Then, the model is in accordance to the LEIS result if the contribution of the second layer is estimated to be 56%, 16%, and 30% for Al, Co, and Cu atoms, respectively. These values are in qualitative agreement with the fact that the TM atoms of the second layer are mostly covered by Al in the first layer, while many second-layer Al atoms are uncovered [see also the final configuration in Fig. 6(h)]. Figures 6(f) and 6(g) show top and side views of the structure-optimized W-(AlCoCu) model. The Cu atoms in the topmost layer relaxed inwards, towards the bulk and at the same time the  $\text{Cu}_5$  pentagon was expanding. Each of these Cu atoms resides in a rather deep fourfold hollow site, with only Al atoms below and a fifth Al neighbor in the surface (the distance to the Cu neighbors in the pentagon is rather large, 3.6 Å, slightly larger than the distance to the Al atom directly below the Cu in the third layer). Maximizing the number of bonds between the transition metal (TM) and Al is typical for Al-TM alloys, and leads to a high stability of these alloys (e.g., superalloys). Thus, arriving at such a configuration provides *a posteriori* justification for replacing the Al atoms with Cu. As a further result of the Cu atoms relaxing inwards, the surface corrugation in STM is mainly due to the Al atoms appearing as protrusions.

Simulated STM images were calculated for all the structure-optimized models and compared with the experimental STM

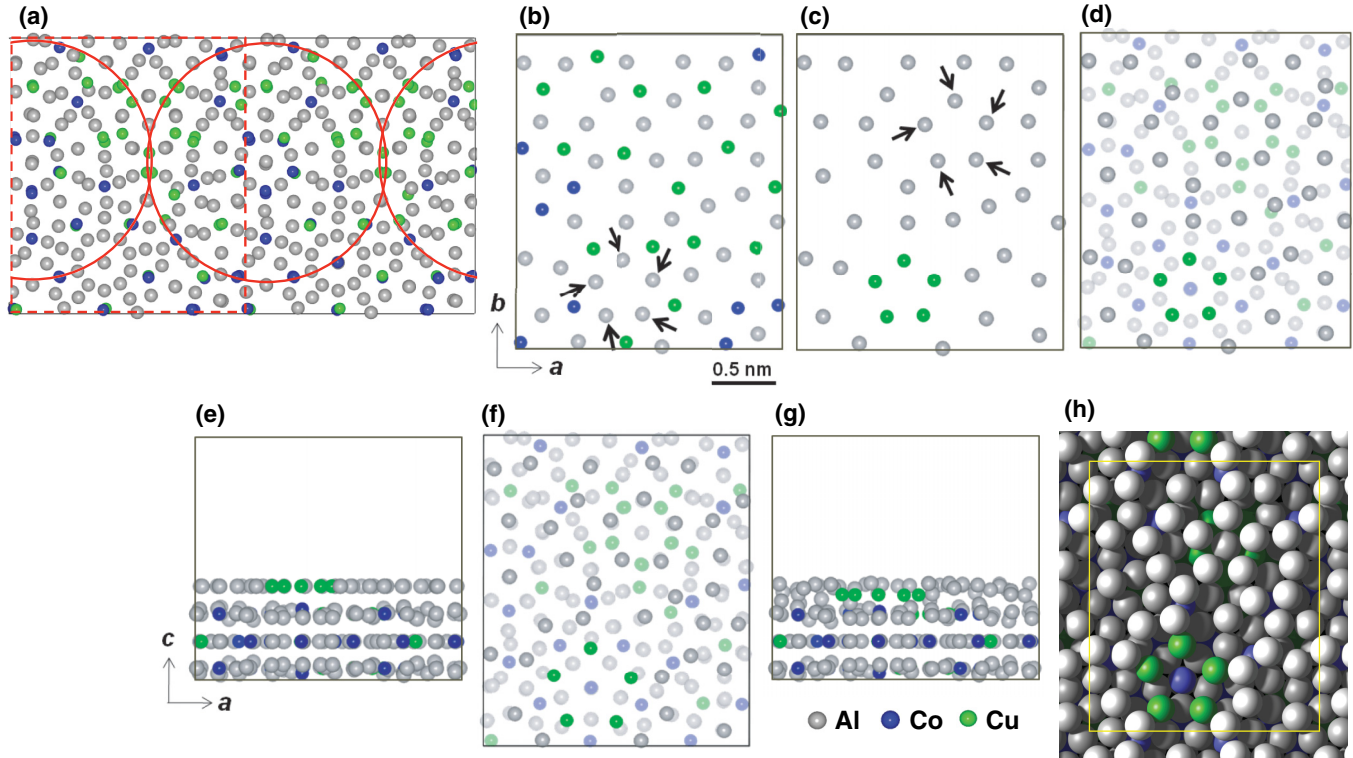


FIG. 6. (Color online) Structure models of the G and Y clusters observed in STM images of d-Al-Co-Cu surface. Al, Co, and Cu atoms are shown as silver, blue, and green balls, respectively. (a) Bulk W-(AlCoCu) approximant. Two 2-nm clusters are marked with solid circles. (b) Truncated A layer of the unmodified W-(AlCoCu) approximant. (c) Compositionally modified topmost layer of the W-(AlCoCu) model. The Al atoms with the arrows in (b) were replaced with Cu atoms in (c). (d) Top view and (e) side view of the initial model. (f) and (h) Top view and (g) side view of the structure-optimized model.

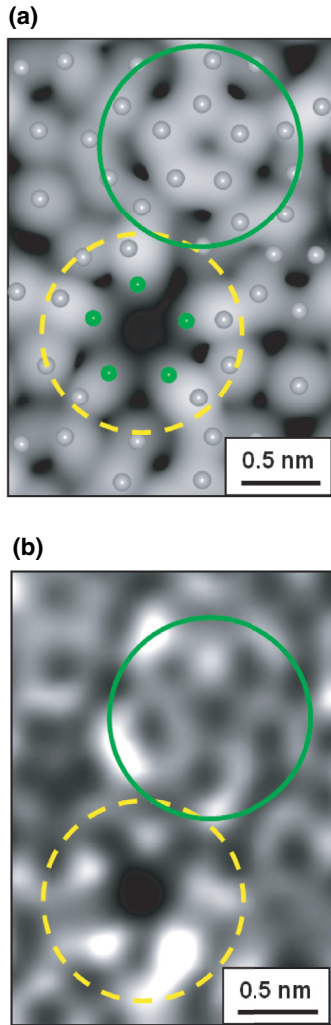


FIG. 7. (Color online) (a) Negative-bias ( $V_s = -0.3$  V) simulated STM image with the atomic arrangement of the topmost layer shown as overlay. (b) Negative-bias ( $V_s = -0.3$  V) experimental STM image of the d-Al-Co-Cu surface.

images. Most of the simulated images, including all structures based on the B layer, do not reproduce the G and Y clusters in the STM images, except the model of the modified A layer shown in Figs. 6(f) and 6(g). Figure 7(a) shows the simulated image of this model with a sample bias of  $-0.3$  V, with the atomic arrangement of the topmost layer superimposed. Figure 7(b) shows a magnified part of the experimental image of Fig. 4(b) (recorded at  $-0.3$  V bias). The circles drawn with solid and broken lines indicate the G and Y clusters in each image. The appearance of the G and Y clusters in the experimental image is clearly reproduced by the simulation; in particular, the Y cluster shows very good agreement. When the Cu pentagon in the topmost layer was eliminated or replaced with an Al or Co pentagon, such a Y cluster did not appear in the simulated image. When the Al pentagon arrowed in Fig. 6(c) was eliminated or replaced with Cu atoms, neither the experimental G nor the Y cluster could match the simulated image around this site. This clearly demonstrates that not only the atomic arrangement of the topmost layer but also chemical species for the second layer are important to reproduce the

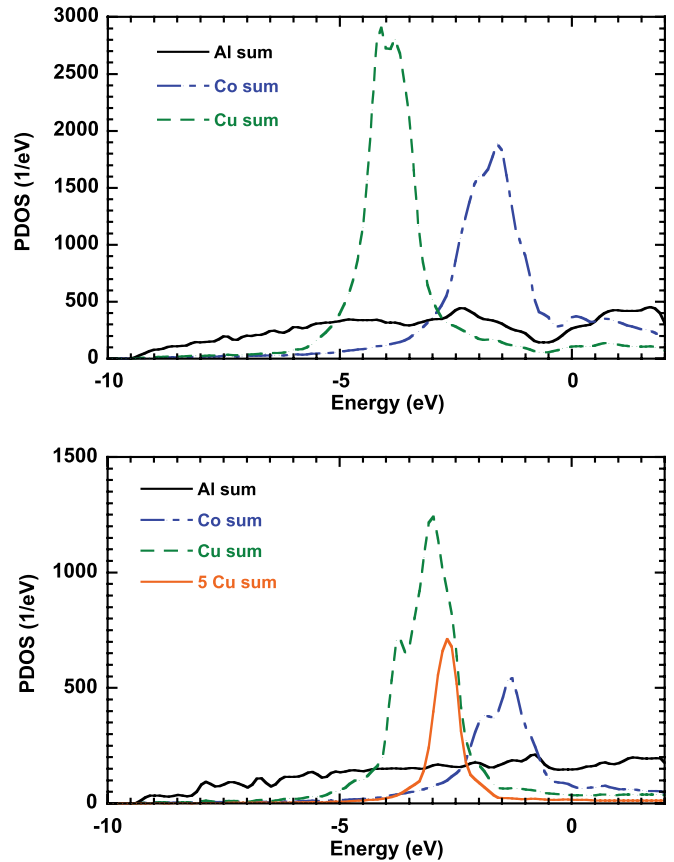


FIG. 8. (Color online) Calculated partial densities of states of (a) the bulk W-(AlCoCu) approximant and (b) the uppermost two layers of the slab representing the d-Al-Co-Cu surface.

appearance of the surface in the STM image: In the correct structural model fitting the experiment, the Cu pentagon in the topmost layer is located on an Al pentagon with a central Co atom (second layer), while the Al pentagon arrowed in Fig. 6(c) is not located around a central second-layer TM metal atom but rather on a Cu pentagon. We also note that the quasicrystal acts as a template for the “soft” Al to form a quasiperiodic structure in the first layer, even in the absence of TM atoms in this layer.

The choice of the final model was based on comparison of the experimental and calculated STM images. Nevertheless, we have also compared the surface energies of all models. The surface energies of our final model and a truncated-bulk model are degenerate within the error bars ( $\approx 5\text{--}10$  meV/ $\text{\AA}^2$ ); all other models are less favorable. The error bars are mainly due to inaccurate chemical potentials of the elements (we have derived the chemical potentials from the bulk energies of the AlCu, Al<sub>2</sub>Cu, Al<sub>5</sub>Co<sub>2</sub>, Al<sub>13</sub>Co<sub>4</sub>, Al<sub>9</sub>Co<sub>2</sub>, AlCo, Al<sub>12</sub>Co<sub>4</sub>Cu, and W-(AlCoCu) phases).

Figure 8 shows the calculated partial densities of states (DOS) of Al, Co, and Cu (a) for the bulk W-(AlCoCu) approximant and (b) of the uppermost two layers of the slab representing the d-Al-Co-Cu surface. The DOSs of both structures are similar except for the peak of the Cu DOS at 3 eV below the Fermi level  $E_F$ . The DOS of the Cu atoms in the pentagonal cluster at the surface is shown as “5 Cu sum;” it peaks at  $E_F - 2.8$  eV. The narrow peak width (i.e.,

narrow  $d$  band) is obviously related to the low coordination of these Cu atoms and the equivalent positions of these five atoms. It is interesting to note that these five Cu atoms are not completely dark in the experimental and simulated STM images (Fig. 7), in spite of being  $\sim 0.7$  Å below the average height of the surface Al, and the low Cu DOS near the Fermi level. We must recall, however, that the DOS peaks of the Cu and Co atoms correspond to  $d$  electrons, which do not reach far into the vacuum, where the STM tip probes the local DOS. To a lesser degree, the same is true for the Al atoms, which have a large  $p$  contribution to the DOS. On the other hand, the DOS of the Cu atoms near  $E_F$  is due to  $s$  states, having the weakest decay with distance from the atomic cores.

As we did not find an agreement between any model of a modified B layer and the experimental STM images of the G and Y clusters, it seems that we have to modify many atoms in this structure to match the STM image. As noted above, the observation of only one type of layer by STM and the absence of any indication of alternating step widths (different surface energies with A or B layer below) cannot be simply explained by having always the same surface layer, but the second layer being either A or B, depending on the terrace level. Instead, this observation must be explained differently: One possibility would be domain boundaries in the bulk, and each step would coincide with the line where a domain boundary meets the surface. In this scenario, the domain-boundary energies would be rather low, so that the surface structure can easily impose the domain structure on the underlying bulk. Another possibility would be a kind of buffer layer (probably consisting of several monolayers) mediating between the uppermost layers and the layers below, where the strict distinction between A and B layers is not present in the buffer layer. This would be a kind of domain boundary parallel to the surface, and again the energy associated with it has to be very low. In all these domain-boundary-type models the domain boundaries must not break the different orientations of adjacent layers, however, because STM always shows that equivalent clusters on adjacent layers are rotated by  $36^\circ$ .<sup>29</sup> Both of these scenarios are comparable to the result of a recent study by Schaub *et al.*, where only a weak correlation over long distances was found.<sup>37</sup>

It is also interesting to compare the present results with those obtained for the surfaces of icosahedral 3D quasicrystals. In the case of Al-Pd-Mn icosahedral quasicrystals, several

papers have proposed that a surface with increased Al content (Al segregation) better explains the experimental results than the bulk-truncated model, although the atomic structure of the topmost surface is rather similar to a truncated bulk.<sup>52-55</sup> Therefore, the Al segregation found in the present work as well as in our previous study of an Al-Ni-Co QC<sup>26</sup> is not a unique case, and we consider it a rule rather than an exception. To further confirm our results, surface studies of QCs using complimentary techniques such as surface x-ray diffraction or high-resolution core level photoemission spectroscopy would be clearly desirable.

#### IV. CONCLUSION

The composition of the d-Al<sub>65</sub>Co<sub>20</sub>Cu<sub>15</sub> near-surface region after annealing was estimated to be Al<sub>77</sub>Co<sub>10</sub>Cu<sub>13</sub>, which is Al richer and Co poorer than the bulk and the surface after sputtering. This observation agrees with the expected surface segregation behavior based on the surface energies of the pure metal constituents. Two types of characteristic clusters, named G and Y clusters, were observed in the STM images at both positive and negative sample bias. The STS spectra of the G and Y clusters revealed only subtle differences of the unoccupied states. Structural optimization using DFT was performed with different models based on the W-(AlCoCu) approximant. The atomic arrangement of the topmost layer was modified according to the composition estimated by the AES and LEIS results. A surface structure with good agreement of the simulated STM image with the experimental ones was identified. This structure is based on a termination with a partially occupied A layer, and it was found that the topmost layer of the G cluster consists of a pentagon of Al atoms, while that of the Y cluster attributed to a pentagon of Cu atoms. The DFT study indicated that the relationship between the topmost and second layers was also important in constructing each cluster.

#### ACKNOWLEDGMENTS

The authors gratefully acknowledge Professor A. P. Tsai and Professor Y. Yokoyama in Tohoku University for providing us quasicrystal specimens. The work in Vienna was supported by the Austrian Science Fund (FWF).

<sup>1</sup>D. Shechtman, I. Blech, D. Gratias, and J. W. Cahn, *Phys. Rev. Lett.* **53**, 1951 (1984).

<sup>2</sup>A. P. Tsai, A. Inoue, and T. Masumoto, *Jpn. J. Appl. Phys.* **26**, L1505 (1987).

<sup>3</sup>A. P. Tsai, A. Inoue, Y. Yokoyama, and T. Masumoto, *Mater. Trans., JIM* **31**, 98 (1990).

<sup>4</sup>A. P. Tsai, A. Inoue, and T. Masumoto, *Mater. Trans., JIM* **30**, 463 (1989).

<sup>5</sup>K. Hiraga, W. Sun, and F. J. Lincoln, *Jpn. J. Appl. Phys.* **30**, L302 (1991).

<sup>6</sup>K. Saitoh, K. Tsuda, and M. Tanaka, *Philos. Mag. A* **76**, 135 (1997).

<sup>7</sup>K. Edagawa, K. Suzuki, and S. Takeuchi, *Phys. Rev. Lett.* **85**, 1674 (2000).

<sup>8</sup>K. Edagawa, P. Mandal, K. Hosono, K. Suzuki, and S. Takeuchi, *Phys. Rev. B* **70**, 184202 (2004).

<sup>9</sup>Y. Yan, S. J. Pennycook, and A. P. Tsai, *Phys. Rev. Lett.* **81**, 5145 (1998).

<sup>10</sup>E. Abe, K. Saitoh, H. Takakura, A. P. Tsai, P. J. Steinhardt, and H.-C. Jeong, *Phys. Rev. Lett.* **84**, 4609 (2000).

<sup>11</sup>E. Abe, S. J. Pennycook, and A. P. Tsai, *Nature* **421**, 347 (2003).

<sup>12</sup>S. Taniguchi and E. Abe, *Philos. Mag.* **88**, 1949 (2008).

<sup>13</sup>W. Steurer and K. H. Kuo, *Acta Crystallogr. Sect. B* **46**, 703 (1990).

- <sup>14</sup>H. Takakura, A. Yamamoto, and A. P. Tsai, *Acta Crystallogr. Sect. A* **57**, 576 (2001).
- <sup>15</sup>S. Ritsch, C. Beeli, H.-U. Nissen, T. Gödecke, M. Scheffer, and R. Lück, *Philos. Mag. Lett.* **78**, 67 (1998).
- <sup>16</sup>B. Grushko, *J. Non-Cryst. Solids* **153**, 489 (1993).
- <sup>17</sup>R. Würschum, T. Troev, and B. Grushko, *Phys. Rev. B* **52**, 6411 (1995).
- <sup>18</sup>W. Bogdanowicz, *Mater. Sci. Eng., A* **372**, 91 (2004).
- <sup>19</sup>K. Saitoh and A. P. Tsai, *Philos. Mag.* **87**, 2741 (2007).
- <sup>20</sup>E. Cockayne and M. Widom, *Phys. Rev. Lett.* **81**, 598 (1998).
- <sup>21</sup>K. Sugiyama, S. Nishimura, and K. Hiraga, *J. Alloys Compd.* **342**, 65 (2002).
- <sup>22</sup>S. Deloudi and W. Steurer, *Philos. Mag.* **87**, 2727 (2007).
- <sup>23</sup>M. Krajčič, J. Hafner, and M. Mihalkovič, *Phys. Rev. B* **73**, 134203 (2006).
- <sup>24</sup>A. R. Kortan, R. S. Becker, F. A. Thiel, and H. S. Chen, *Phys. Rev. Lett.* **64**, 200 (1990).
- <sup>25</sup>M. Kishida, Y. Kamimura, R. Tamura, K. Edagawa, S. Takeuchi, T. Sato, Y. Yokoyama, J. Q. Guo, and A. P. Tsai, *Phys. Rev. B* **65**, 094208 (2002).
- <sup>26</sup>J. Yuhara, J. Klikovits, M. Schmid, P. Varga, Y. Yokoyama, T. Shishido, and K. Soda, *Phys. Rev. B* **70**, 024203 (2004).
- <sup>27</sup>H. R. Sharma, K. J. Franke, W. Theis, A. Riemann, S. Fölsch, P. Gille, and K. H. Rieder, *Phys. Rev. B* **70**, 235409 (2004).
- <sup>28</sup>T. Duguet, B. Únal, M. C. de Weerd, J. Ledieu, R. A. Ribeiro, P. C. Canfield, S. Deloudi, W. Steurer, C. J. Jenks, J. M. Dubois, V. Fournée, and P. A. Thiel, *Phys. Rev. B* **80**, 024201 (2009).
- <sup>29</sup>R. Zenkyu, T. Matsui, A. P. Tsai, and J. Yuhara, *Philos. Mag.* **91**, 2854 (2011).
- <sup>30</sup>J. Yuhara, M. Sato, T. Matsui, and A. P. Tsai, *Philos. Mag.* **91**, 2846 (2011).
- <sup>31</sup>Ph. Ebert, F. Kluge, M. Yurechko, B. Grushko, and K. Urban, *Surf. Sci.* **523**, 298 (2003).
- <sup>32</sup>N. Ferralis, K. Pussi, E. J. Cox, M. Gierer, J. Ledieu, I. R. Fisher, C. J. Jenks, M. Lindroos, R. McGrath, and R. D. Diehl, *Phys. Rev. B* **69**, 153404 (2004).
- <sup>33</sup>K. Pussi, N. Ferralis, M. Mihalkovic, M. Widom, S. Curtarolo, M. Gierer, C. J. Jenks, P. Canfield, I. R. Fisher, and R. D. Diehl, *Phys. Rev. B* **73**, 184203 (2006).
- <sup>34</sup>Katariina Pussi and Renee D. Diehl, *Z. Kristallogr.* **224**, 1 (2009).
- <sup>35</sup>V. Blum, L. Hammer, W. Meier, and K. Heinz, *Surf. Sci.* **488**, 219 (2001).
- <sup>36</sup>S. E. Burkov, *Phys. Rev. Lett.* **67**, 614 (1991).
- <sup>37</sup>P. Schaub, T. Weber, and W. Steurer, *J. Appl. Cryst.* **44**, 134 (2011).
- <sup>38</sup>J. Q. Guo, E. Abe, T. J. Sato, and A. P. Tsai, *Jpn. J. Appl. Phys.* **38**, L1049 (1999).
- <sup>39</sup>Y. Yokoyama, R. Note, A. Yamaguchi, A. Inoue, K. Fukaura, and H. Sunada, *Mater. Trans., JIM* **40**, 123 (1999).
- <sup>40</sup>L. E. Davis, N. C. MacDonald, P. W. Palmberg, G. E. Riach, and R. E. Weber, *Handbook of Auger Electron Spectroscopy*, 2nd ed. (Physical Electronics Industries, Eden Prairie, MN, 1976).
- <sup>41</sup>W. Smekal, W. S. M. Werner, and C. J. Powell, *Surf. Interface Anal.* **37**, 1059 (2005).
- <sup>42</sup>W. S. M. Werner, *Surf. Interface Anal.* **31**, 141 (2001).
- <sup>43</sup>M. Mihalkovič and M. Widom, alloy database at <http://alloy.phys.cmu.edu/>.
- <sup>44</sup>G. Kresse and J. Furthmüller, *Phys. Rev. B* **54**, 11169 (1996).
- <sup>45</sup>G. Kresse and D. Joubert, *Phys. Rev. B* **59**, 1758 (1999).
- <sup>46</sup>J. P. Perdew and Y. Wang, *Phys. Rev. B* **45**, 13244 (1992).
- <sup>47</sup>J. Tersoff and D. R. Hamann, *Phys. Rev. B* **31**, 805 (1985).
- <sup>48</sup>R. Kelly, *Surf. Interface Anal.* **7**, 1 (1985).
- <sup>49</sup>P. Sigmund, *Nucl. Instrum. Methods Phys. Res., Sect. B* **27**, 1 (1987).
- <sup>50</sup>R. Kelly, *Nucl. Instrum. Methods Phys. Res., Sect. B* **13**, 283 (1986).
- <sup>51</sup>H. H. Brongersma, M. Draxler, M. de Ridder, and P. Bauer, *Surf. Sci. Rep.* **62**, 63 (2007).
- <sup>52</sup>L. Barbier, D. Le Floc'h, Y. Calvayrac, and D. Gratias, *Phys. Rev. Lett.* **88**, 085506 (2002).
- <sup>53</sup>C. J. Jenks, A. R. Ross, T. A. Lograsso, J. A. Whaley, and R. Bastasz, *Surf. Sci.* **521**, 34 (2002).
- <sup>54</sup>J.-C. Zheng, C. H. A. Huan, A. T. S. Wee, M. A. Van Hove, C. S. Fadley, F. J. Shi, E. Rotenberg, S. R. Barman, J. J. Paggel, K. Horn, Ph. Ebert, and K. Urban, *Phys. Rev. B* **69**, 134107 (2004).
- <sup>55</sup>M. Gierer, M. A. Van Hove, A. I. Goldman, Z. Shen, S.-L. Chang, P. J. Pinhero, C. J. Jenks, J. W. Andereg, C.-M. Zhang, and P. A. Thiel, *Phys. Rev. B* **57**, 7628 (1998).